

Numerical study of detonation wave propagation modes in annular channels

Cite as: AIP Advances 11, 085203 (2021); <https://doi.org/10.1063/5.0057586>

Submitted: 22 May 2021 • Accepted: 20 July 2021 • Published Online: 03 August 2021

Duo Zhang,  Xueqiang Yuan, Shijie Liu, et al.

COLLECTIONS

Paper published as part of the special topic on [Fluids and Plasmas](#)



View Online



Export Citation



CrossMark

ARTICLES YOU MAY BE INTERESTED IN

[Computational study of gaseous cellular detonation diffraction and re-initiation by small obstacle induced perturbations](#)

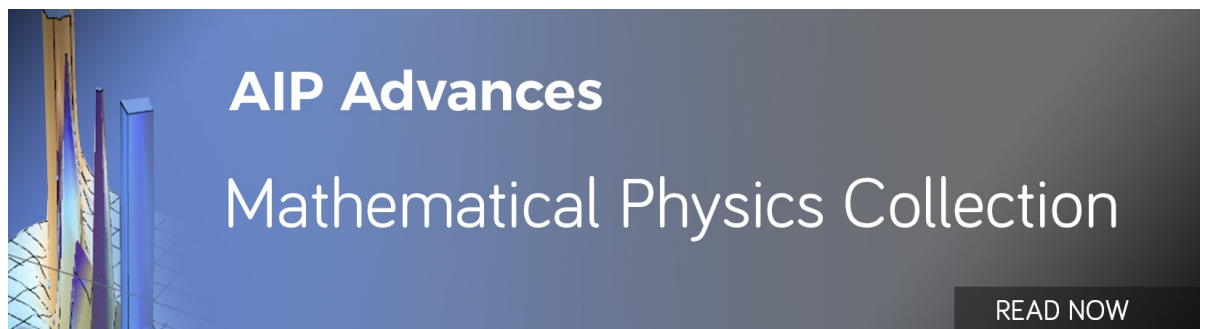
Physics of Fluids **33**, 047115 (2021); <https://doi.org/10.1063/5.0044164>

[Three-dimensional simulations of detonation propagation in circular tubes: Effects of jet initiation and wall reflection](#)

Physics of Fluids **32**, 046104 (2020); <https://doi.org/10.1063/1.5143105>

[Modeling thermodynamic trends of rotating detonation engines](#)

Physics of Fluids **32**, 126102 (2020); <https://doi.org/10.1063/5.0023972>



AIP Advances
Mathematical Physics Collection

READ NOW

Numerical study of detonation wave propagation modes in annular channels

Cite as: AIP Advances 11, 085203 (2021); doi: 10.1063/5.0057586

Submitted: 22 May 2021 • Accepted: 20 July 2021 •

Published Online: 3 August 2021



View Online



Export Citation



CrossMark

Duo Zhang,¹ Xueqiang Yuan,^{1,a)}  Shijie Liu,¹ Xiaodong Cai,¹  Haoyang Peng,¹ Ralf Deiterding,² 
and Hoi Dick Ng³ 

AFFILIATIONS

¹Science and Technology on Scramjet Laboratory, National University of Defense Technology, Changsha 410073, China

²Aerodynamics and Flight Mechanics Research Group, School of Engineering, University of Southampton, Southampton SO16 7QF, United Kingdom

³Department of Mechanical, Industrial and Aerospace Engineering, Concordia University, Montréal, Québec H3G 1M8, Canada

^{a)}Author to whom correspondence should be addressed: yuanxueqiang09@nudt.edu.cn

ABSTRACT

Modes of detonation wave propagation in annular channels were investigated numerically by using the adaptive mesh refinement technique. Two-dimensional, reactive Euler equations with a detailed hydrogen/oxygen reaction model were adopted in the computations to simulate the detonation dynamics in the annular geometry. Considering both the decoupling of the detonation wave front and the development of the Mach-stem in reflection, the propagation is divided into unstable and stable propagation modes with different Mach-stem evolutions, namely, a growing, steady, or decaying type. The numerical observations indicate that in the unstable propagation mode, velocity loss and oscillation occur near the inner wall, while the wave front shape and velocity evolution are steadier for the stable propagation mode. The overdriven degree near the outer wall increases as the Mach-stem strength attenuates. The propagation mode diagrams demonstrate that an increase in the initial pressure and wall curvature radius can extend the range of the stable propagation mode, and the Mach-stem is transformed from a growing to steady, and finally a decaying type with the increase in the initial pressure or the decrease in the wall curvature radius to channel width ratio. The limit of wall curvature radius separating the unstable and stable modes is independent of the channel width for the Mach-stem steady and decaying types, while they are positively correlated for the Mach-stem growing type. Finally, a qualitative procedure is proposed to help distinguish different propagation modes based on the formation mechanism of each propagation dynamics.

© 2021 Author(s). All article content, except where otherwise noted, is licensed under a Creative Commons Attribution (CC BY) license (<http://creativecommons.org/licenses/by/4.0/>). <https://doi.org/10.1063/5.0057586>

I. INTRODUCTION

A rotating detonation engine (RDE) is a detonation-based propulsion device that can realize continuous detonative combustion in the chamber and provide high-frequency stable thrust. The self-pressurization characteristic and high thermodynamic efficiency make the RDE become the principal focus in the recent development of hypersonic propulsion systems.^{1–4} In the annular combustion chamber of the RDE, the detonation wave experiences lateral expansion in the axial direction as well as the effects of two cylindrical chamber walls in the radial direction. Recent studies have claimed that the radial sizes of the chamber are significant parameters in affecting the performance and steady operation of the engine, which can cause the failure or unstable propagation of the

detonation wave.⁵ To investigate the role of the two radial wall boundaries of a RDE, the propagation of the detonation wave in the circumferential direction can be approximated as that through a quiescent gas mixture in the annular channel. In essence, the study of detonation wave propagation in the annular channel can provide significant guidance for the design of the combustion chamber of the RDE.

Due to the complex influence of both the inner and outer walls, the detonation wave can exhibit specific propagation modes in the annular channel. Thomas and Williams⁶ found that the detonation wave could propagate stably in the channel with detonation cells compressed near the outer wall and enlarged near the inner wall, while an unstable propagation could also be formed in some cases with the appearance of detonation failure and re-initiation

alternatively. The re-initiation process was studied numerically by Deiterding *et al.*,^{7,8} Li *et al.*,⁹ and Yuan *et al.*,¹⁰ reporting that the flow state behind the Mach-stem can ignite the unburned mixture in the decoupled area, which is the key factor in arising the detonation re-initiation, while Melguizo-Gavilanes *et al.*¹¹ explained the re-initiation phenomenon from the view of global dynamics, denoting that the formation of re-initiation is mainly determined by the channel geometry and initial pressure, instead of the highly compressed region behind the Mach-stem. Ioannou *et al.*¹² studied the detonation propagation in annular arcs of condensed phase explosives, finding that the detonation wave goes through a transition phase and eventually reaches a new steady state of constant angular velocity.

The numerical study of Lee *et al.*¹³ indicated that the detonation propagation mode was closely related to the channel radius of curvature. Only the radius larger than a critical value could result in a stable propagation. The unstable and stable propagation modes were clarified in the experimental study of Kudo *et al.*¹⁴ according to whether the detonation wave front was decoupled, and the critical curvature radius of the inner wall for propagation mode transition was found to be 14λ , where λ represents the width of the detonation cell. Nakayama *et al.*^{15–17} refined the propagation modes based on the study of Kudo *et al.*, suggesting that a critical mode existed between the unstable and stable modes, and the critical inner wall radii for the transition of these modes are 14λ and 23λ , respectively. This conclusion was verified by Pan *et al.*,^{18,19} and they also provided that the critical radius for detonation formation was about 2.6–2.8 λ . Considering that the critical radii above are obtained by statistical analysis of the results, Sugiyama *et al.*²⁰ engaged to determine the critical criterion by applying the $D_n - \kappa$ theory. Short *et al.*²¹ and Xia *et al.*²² observed some new propagation modes, such as a stable propagation mode with the co-existence of the curved detonation wave front and Mach-stem, which enriched the research of the detonation propagation mode in the annular channel.

Although the detonation wave propagation in the annular channel has been widely studied, the entire propagation modes as well as their characteristics and formation mechanisms have not been investigated systematically and adequately. Following the aforementioned studies, all the modes of detonation wave propagation in annular channels were investigated numerically in the present work. Key features for different detonation propagation modes have been described in detail, focusing on both the decoupling of the diffracted detonation wave near the inner wall and the development of the reflection Mach-stem near the outer wall. The formation mechanism, wave structure, and velocity characteristics of each propagation mode were analyzed, and the dependence of these propagation modes on different geometrical parameters and initial conditions has been clarified. Based on these results, a qualitative procedure is constructed to determine the different modes of detonation propagation in the annular chamber of an RDE.

II. NUMERICAL METHOD AND COMPUTATIONAL SETUP

A. Numerical method

The simulations of cellular detonation wave propagation in annular channels were conducted in a two-dimensional computational domain, as shown in Fig. 1. It represents a semi-annular

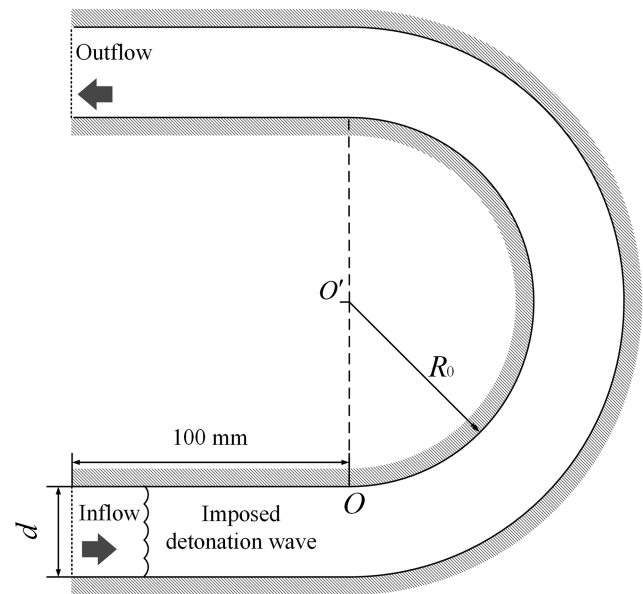


FIG. 1. Schematic of the computational domain.

channel, which connects with straight parts at both the inlet and outlet domains, respectively. A reflecting boundary with the slip condition was used on the inner and outer walls, and a transmissive condition was adopted on the inlet and outlet boundaries. The stoichiometric H_2/O_2 mixture with 70% argon dilution at a temperature of 298 K was distributed in the domain. A detailed chemical reaction model of 9 species and 34 elementary reactions²³ was employed. A self-sustained cellular detonation under specific initial conditions and the corresponding channel width was simulated first and imposed near the inlet domain to initialize the computation. In the present study, the channel width d varied from 20 to 100 mm, and the curvature radius of the inner wall R_0 varied from 20 to 200 mm. Both of them increased with an interval of 20 mm. The chosen initial pressure values p_0 and their corresponding detonation cell width λ are listed in Table I.

The adaptive mesh refinement code AMROC,²⁴ which is an open-source code based on the structured adaptive mesh refinement technique,²⁵ was adopted to capture the fine wave structure of the propagating detonation front in the simulations. The code supports abundant Euler solvers based on total variation diminishing (TVD) and weighted essentially non-oscillatory (WENO) schemes and has been widely applied in multi-dimensional detonation simulations.^{7,8,10,26–29} In the present work, the two-dimensional, reactive Euler equations were used as the governing equations, and

TABLE I. Initial pressure p_0 and the corresponding detonation cell size λ from the simulations.

p_0 (kPa)	λ (mm)
6.5	10
11	6.67
17	4
25	2.5

a second-order accurate monotonic upwind scheme for conservation laws (MUSCL)-TVD finite volume method was adopted. It is worth denoting that to have higher accuracy, the Navier–Stokes and kinetic models^{30–32} can be employed as well. The reaction source

term was handled by the first-order accurate Godunov splitting method. A difference scheme with second-order accuracy in space and time was constructed by the Van Albada limiter with MUSCL reconstruction and the Runge–Kutta technique,³³ respectively. All

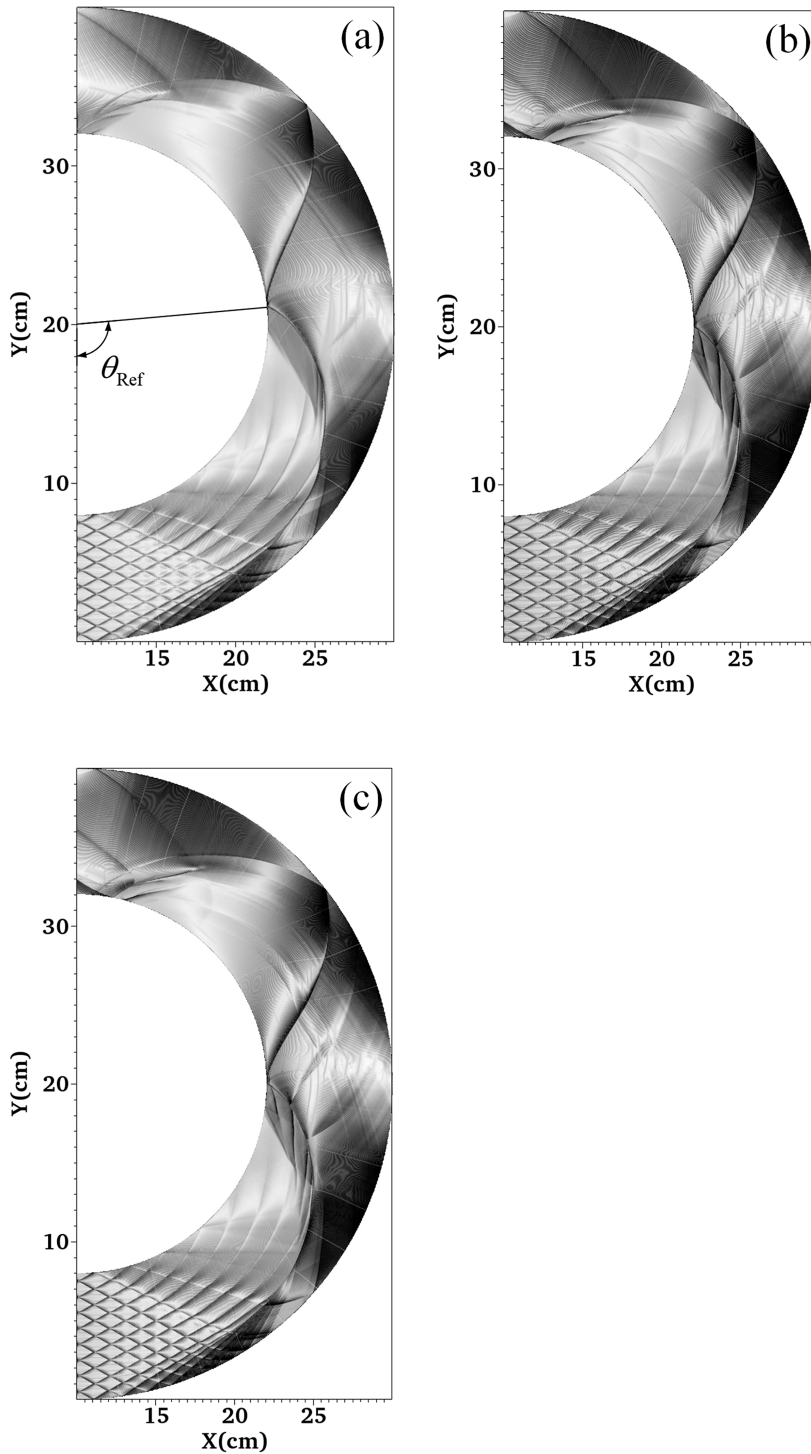


FIG. 2. Numerical soot foils showing the cellular detonation wave propagation in an annular channel for different mesh resolutions: (a) $l_g/\Delta x_{\min} = 8$, (b) $l_g/\Delta x_{\min} = 16$, and (c) $l_g/\Delta x_{\min} = 32$.

simulations used the adjustment of dynamic time steps with a maximum Courant–Friedrichs–Lewy number of 0.95, while the specific value of the number will be changed automatically according to the variation of the space and time step.

B. Grid resolution study and result validation

To investigate the effect of numerical grid resolution on the simulations, a series of verification cases for detonation wave propagation with different mesh refinement strategies were conducted with the conditions of $p_0 = 6.5$ kPa, $d = 80$ mm, and $R_0 = 120$ mm. In this paper, the cellular patterns and trajectory of the reflection triple-point are significant for analyzing the propagation process, so the accuracy of these parameters should be ensured primarily.

TABLE II. Central angle θ_{Ref} where the triple-point first collides with the inner wall for different mesh resolutions.

Resolutions	θ_{Ref} (deg)
$l_{\text{ig}}/\Delta x_{\text{min}} = 8$	93.58
$l_{\text{ig}}/\Delta x_{\text{min}} = 16$	90.81
$l_{\text{ig}}/\Delta x_{\text{min}} = 32$	90.03

Figure 2 presents the numerical soot foils for three different resolutions, where $l_{\text{ig}}/\Delta x_{\text{min}}$ represents the number of grid points per induction length of the corresponding steady ZND detonation in the highest refinement area, and Table II lists the central angle θ_{Ref}

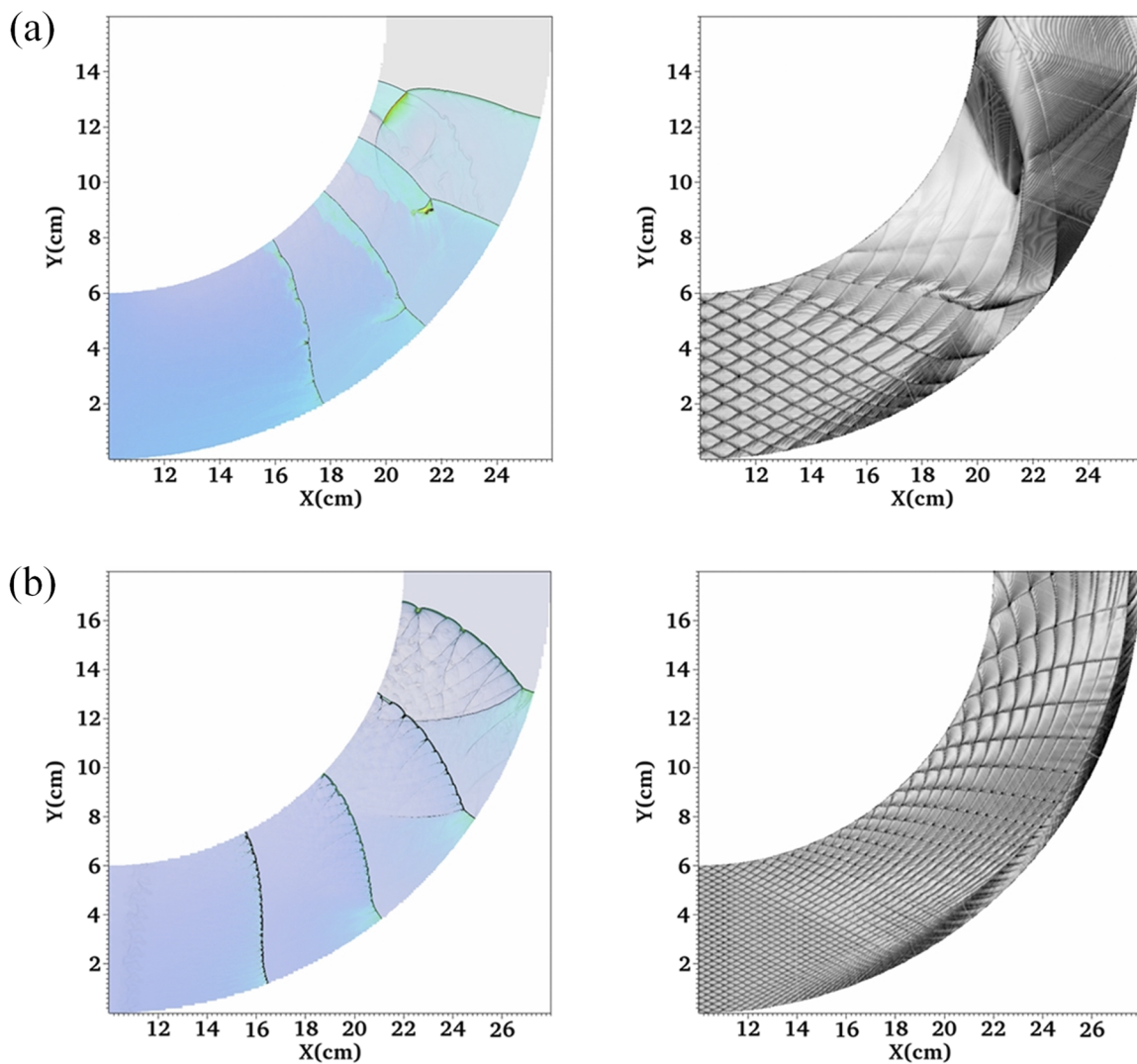


FIG. 3. Density schlieren and numerical soot foil for (a) unstable propagation mode ($p_0 = 11$ kPa, $d = 60$ mm, and $R_0 = 100$ mm) and (b) stable propagation mode ($p_0 = 25$ kPa, $d = 60$ mm, and $R_0 = 120$ mm).

where the reflection triple-point first collides with the inner wall for each resolution. It can be observed that the soot foils are insensitive to the chosen grid resolutions, and the angle θ_{Ref} of all the cases is essentially the same. Considering the computational cost, the resolution of $l_{\text{ig}}/\Delta x_{\text{min}} = 16$ was applied for all the following simulations.

III. RESULTS AND ANALYSIS

In previous studies,^{14,15} the detonation propagation can generally be divided into either unstable or stable propagation modes according to whether the detonation wave front is decoupled or not. A sequence of numerical density schlieren images and the corresponding numerical soot foil for each mode are presented in Fig. 3. The time interval between each two wave fronts in the overlay is

equivalent. In the unstable propagation mode, the decoupling of the detonation wave front occurs during the propagation, and detonation cells disappear on the corresponding cell pattern as shown in Fig. 3(a), whereas in the stable propagation mode, the detonation wave front remains coupled in the entire evolution, with no disappearance of cellular patterns in the numerical soot foil [see Fig. 3(b)]. In fact, from the perspective of the geometrical effect of the annular channel on the detonation wave, whether the detonation wave can propagate stably mainly depends on the diffraction process induced by the inner wall, while the influence of the reflection effect near the outer wall is completely ignored. In order to describe the detonation wave propagation and characteristics in the annular channels more accurately, the present work further subdivides the existing two propagation modes into three types according to the variation of the reflection event near the outer wall, i.e., a growing, steady, and

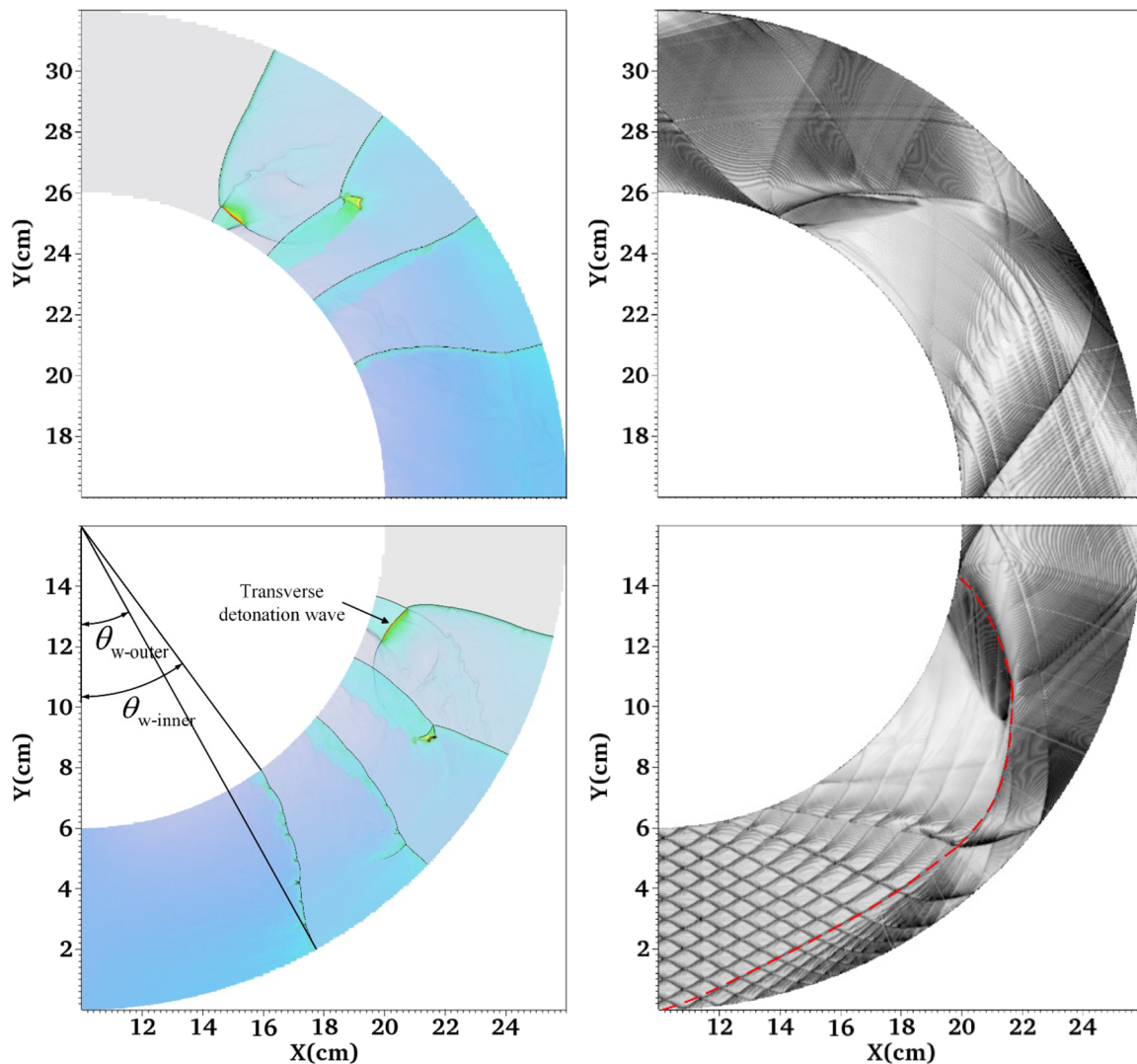


FIG. 4. Density schlieren and numerical soot foil for UPGM mode (red dashed line: the trajectory of the Mach reflection triple-point).

decaying Mach-stem type. The formation mechanism, wave structure, and velocity evolution of these six propagation modes were analyzed in detail.

A. Unstable propagation modes

1. Unstable propagation with growing Mach-stem mode

The density schlieren overlay and soot foil for the unstable propagation with growing Mach-stem (UPGM) mode are displayed in Fig. 4, with the conditions of $p_0 = 11$ kPa, $d = 60$ mm, and $R_0 = 100$ mm. From the density schlieren, the detonation wave front is decoupled by the diffraction effect near the inner wall, while the Mach reflection triple-point near the outer wall contacts with the decoupled front. Since the compression of the outer wall causes a high temperature and pressure zone behind the triple-point, the premixed gas in the decoupled area can be ignited promptly, thus forming a local detonation that propagates transversely along with the reflection triple-point, which was called transverse detonation wave in the previous studies,^{9,10,34} and promoting the height of the Mach-stem to grow rapidly. The numerical soot foil elucidating the structure characteristics of this mode shows that the detonation transverse waves basically disappear, whereas a dominant Mach reflection triple-point exists and collides between the inner and outer walls, leaving an evident moving trajectory (red dashed line). Some cell-like structure can also be observed under the trajectory, which is caused by the propagation of the transverse detonation wave.

Figure 5 presents the velocity evolution of the leading wave front on both the inner and outer walls for the UPGM mode, varying with the central angle θ_w where the wave front locates, as Fig. 4 shows, and the difference between the angles $\theta_{w\text{-inner}}$ and $\theta_{w\text{-outer}}$ is defined as the phase difference of the wave. The velocity D is non-dimensionalized by dividing the Chapman–Jouguet

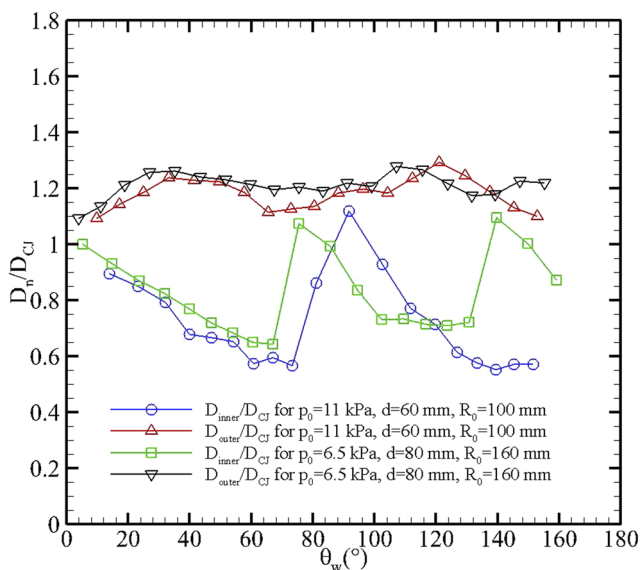


FIG. 5. Velocity evolution on inner and outer walls for the UPGM mode.

detonation velocity D_{CJ} . Due to the detonation diffraction and wave front decoupling near the inner wall, the inner wall velocity D_{inner} is much lower than D_{CJ} at most of the positions and has a decreasing tendency along with θ_w . However, there is a significant sharp rise when the Mach reflection triple-point moves toward the inner wall, and the velocity reaches the highest where the triple-point collides with the wall. The interaction with this triple-point recouples the diffracted wave front and enhances the detonation strength. Moreover, the entire detonation wave front is coupled when the triple-point reaches the wall, thus corresponding to the highest velocity. By contrast, the velocity evolution on the outer wall is relatively stable, and globally higher than 1, indicating that the detonation wave is in an overdriven state. An explanation is that the velocity perpendicular to the wave front of the reflection triple-point, which is a component of the triple-point velocity D_R , approximates to D_{CJ} , as Fig. 6 shows. Assuming the Mach-stem is straight and perpendicular to the outer wall, the velocity of the wave front on the outer wall D_{outer} equals to D_R , thereby causing D_{outer} higher than D_{CJ} .

2. Unstable propagation with steady Mach-stem mode

Figure 7 shows the detonation wave structure and cellular pattern variation in the unstable propagation with steady Mach-stem (UPSM) mode. The corresponding conditions are $p_0 = 17$ kPa, $d = 80$ mm, and $R_0 = 120$ mm. Compared with the UPGM mode, this propagation mode occurs at a higher initial pressure, so the diffracted detonation wave near the inner wall can realize reinitiation spontaneously, with a limited decoupled area on the wave front. On the other hand, due to the smaller ratio R_0/d in this case, the tendency of the reflection triple-point moving toward the inner wall is weakened. Therefore, no contact between the decoupling area and the reflection triple-point occurs, and the growth of the Mach-stem cannot be promoted. When the angle between the wave front and the outer wall θ_d varies in a certain range, an essentially

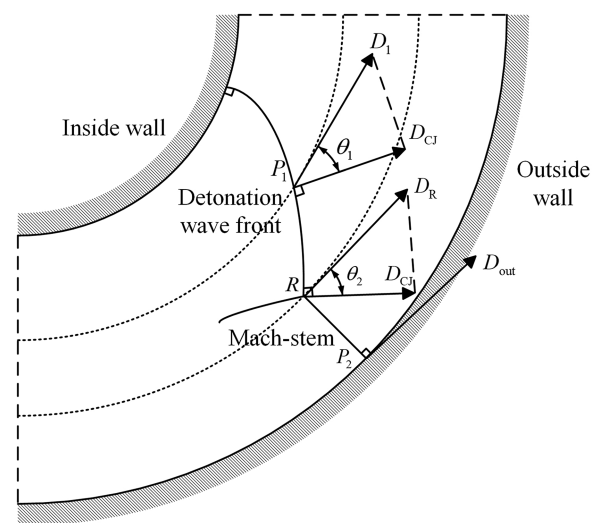


FIG. 6. Schematic showing velocity distribution of the detonation wave front in the annular channel.

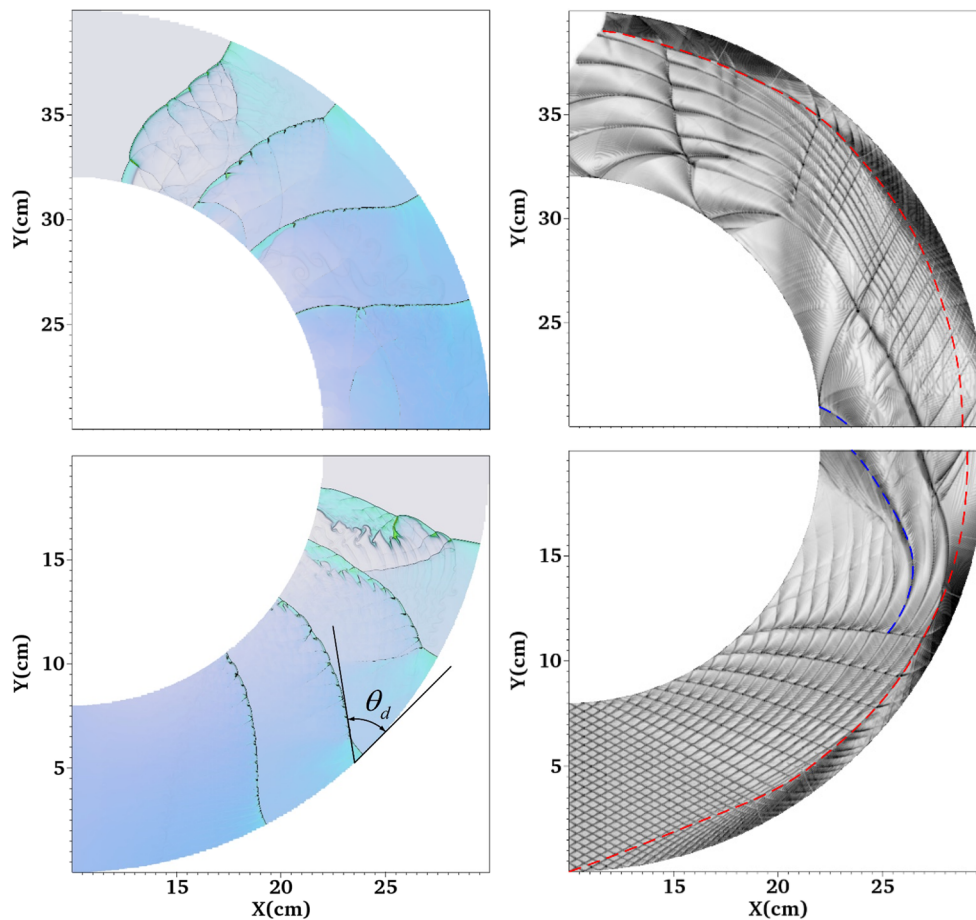


FIG. 7. Density schlieren and numerical soot foil for the UPSM mode (red dashed line: the trajectory of the Mach reflection triple-point; blue dashed line: the trajectory of the transverse detonation wave generated by the re-initiation).

unchanged Mach-stem is formed. An important characteristic of this mode is that the re-initiation of the diffracted detonation wave and the development of the Mach-stem are completely independent, so there are two primary trajectories in the soot foil, each corresponds to the movement of the transverse detonation wave generated by the re-initiation (blue dashed line) and that of the Mach reflection triple-point (red dashed line), respectively. The cellular structure at the left side of the blue line disappears, indicating that the wave front decouples, while the cell sizes at the right side of the red line are much smaller due to the compression of the reflection. In addition, the trajectory of the triple-point does not intersect with the inner or outer wall.

The velocity evolution for the UPSM mode is shown in Fig. 8. The variation is similar to that of the UPGM mode. For the inner wall, the diffraction and decoupling of the detonation wave also cause the global velocity D_{inner} far below D_{CJ} , and a sharp velocity rise also occurs with the maximum velocity ratio $D_{\text{inner}}/D_{\text{CJ}}$ reaching 1.1. The difference is that the velocity rise is caused by the collision between the inner wall and the transverse detonation wave for the re-initiation, instead of the reflection triple-point, while the

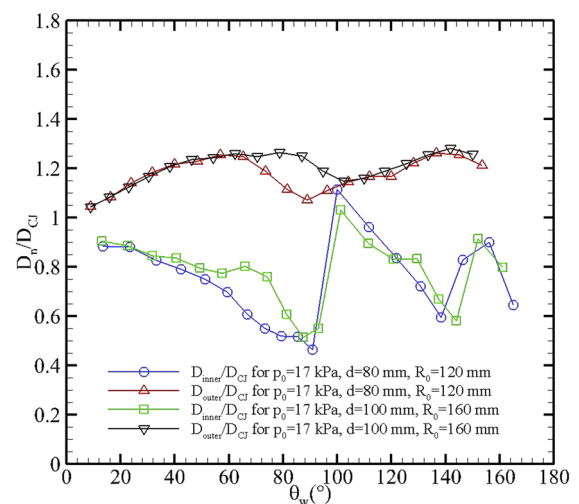


FIG. 8. Velocity evolution on inner and outer walls for the UPSM mode.

velocity ratio on the outer wall $D_{\text{outer}}/D_{\text{CJ}}$ varies in the range of 1–1.3.

3. Unstable propagation with decaying Mach-stem mode

The formation mechanism of the unstable propagation with decaying Mach-stem (UPDM) mode is similar to that of the UPDM mode. The results are given in Fig. 9 for the case with $p_0 = 25$ kPa, $d = 60$ mm, and $R_0 = 40$ mm. The high initial pressure favors the re-initiation of the diffracted detonation wave, but the decoupling area still exists. Meanwhile, the decrease of the ratio R_0/d not only causes no contact between the decoupling area and the reflection triple-point, but also decreases the angle between the wave front and the outer wall θ_d , thus making the Mach-stem attenuate as it continues

to propagate. Finally, the Mach-stem disappears completely, indicating that the Mach reflection is transformed to the regular reflection. From the soot foil, the trajectory of the transverse detonation wave collides with the inner wall and reflects (blue dashed line), denoting the re-initiation process completes, while the trajectory of the reflection triple-point disappears gradually (red dashed line).

The velocity evolution for the UPDM mode is shown in Fig. 10. As a result of the collision between the transverse detonation wave and the inner wall in the re-initiation process, the wave front velocity ratio on the inner wall $D_{\text{inner}}/D_{\text{CJ}}$ jumps to 1.1, while the diffraction process still causes a decrease of $D_{\text{inner}}/D_{\text{CJ}}$ along with θ_w , and the average velocity ratio is about 0.7. The velocity on the outer wall D_{outer} is much larger than D_{CJ} when stabilized, and the maximum velocity ratio $D_{\text{outer}}/D_{\text{CJ}}$ even reaches 1.6. Such a high overdriven

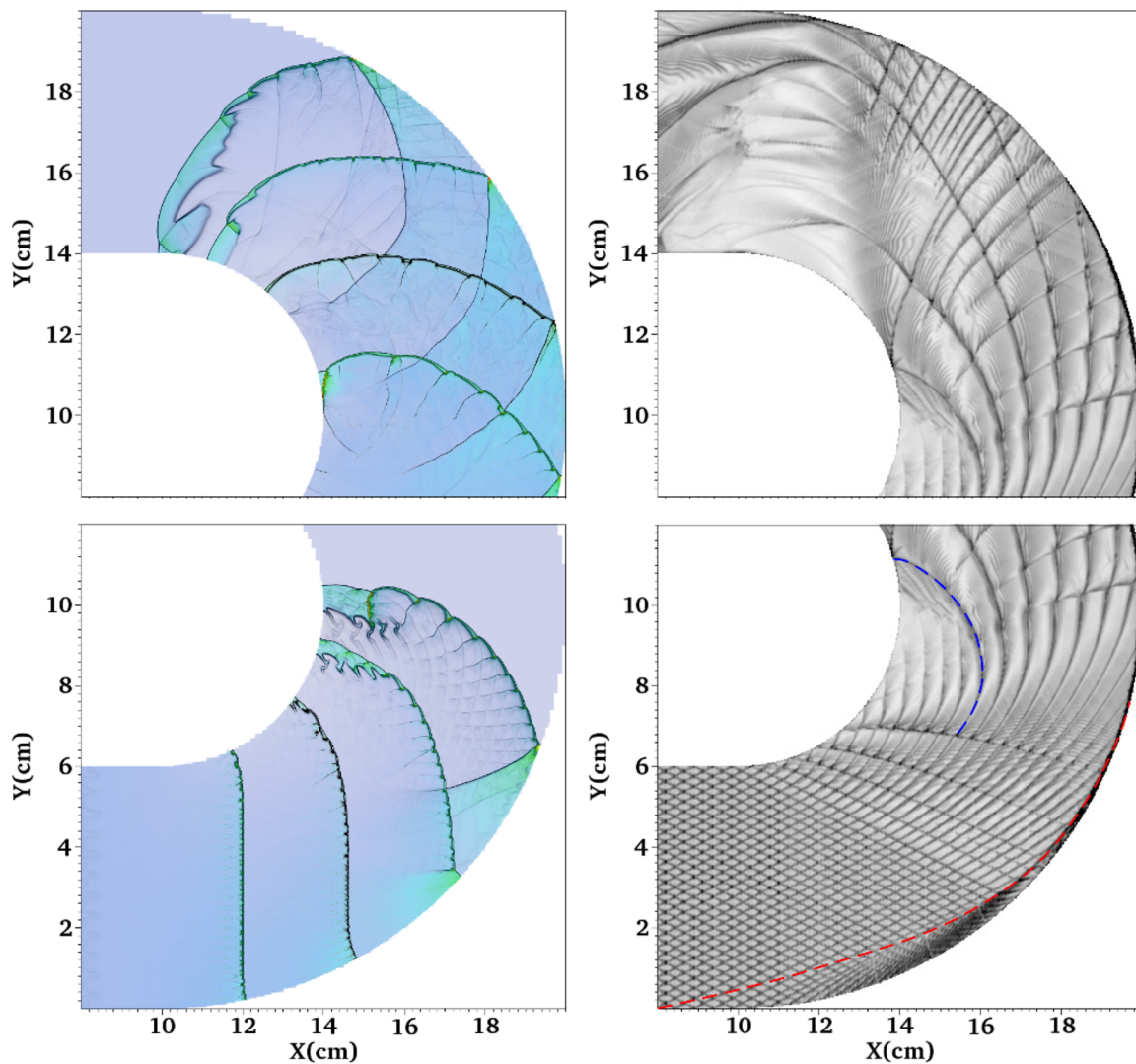


FIG. 9. Density schlieren and numerical soot foil for the UPDM mode (red dashed line: the trajectory of the Mach reflection triple-point; blue dashed line: the trajectory of the transverse detonation wave).

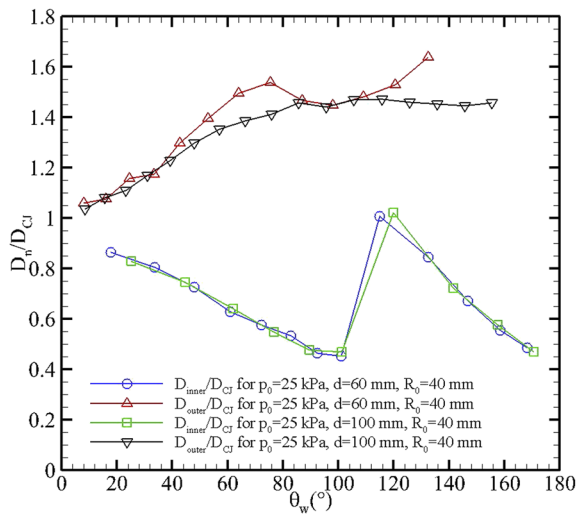


FIG. 10. Velocity evolution on inner and outer walls for the UPDM mode.

state is the consequence of the transition from the Mach reflection to regular reflection, which makes the wave front angle θ_d much smaller than that between the Mach-stem and the outer wall in the Mach reflection.

B. Stable propagation modes

1. Stable propagation with growing Mach-stem mode

The density schlieren overlay and soot foil for the stable propagation with growing Mach-stem (SPGM) mode are displayed in Fig. 11. The conditions are $p_0 = 11$ kPa, $d = 20$ mm, and $R_0 = 140$ mm. The previous study²⁸ has reported that the detonation wave can sustain coupling for a certain distance when diffracting along a curved convex wall, and it can even propagate stably without decoupling as the curvature radius of the convex wall increases to a certain value. Therefore, the formation mechanism of this mode should be elucidated possibly in two situations: (1) even the diffracted detonation wave near the inner wall eventually decouples, a quasi-coupling still holds at the beginning of the diffraction process. Meanwhile, a large R_0 can increase the height of the Mach-stem

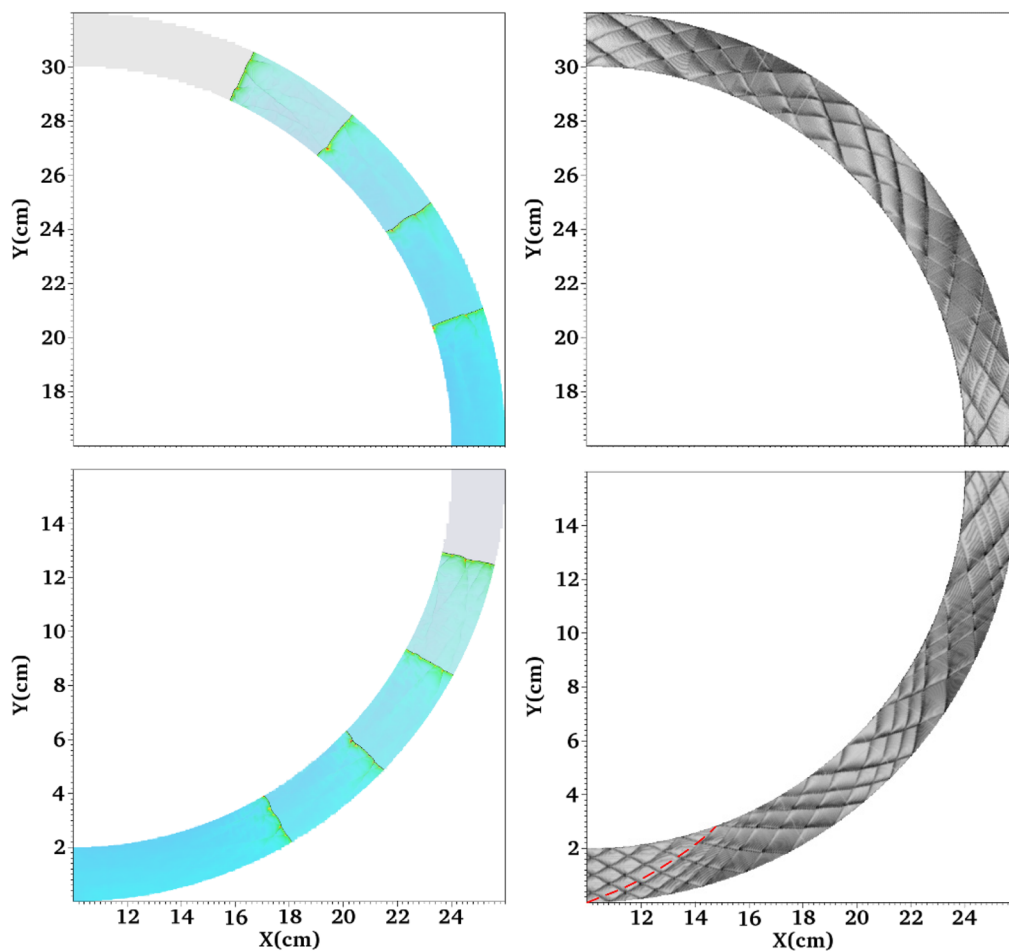


FIG. 11. Density schlieren and numerical soot foil for the SPGM mode (red dashed line: the trajectory of the Mach reflection triple-point).

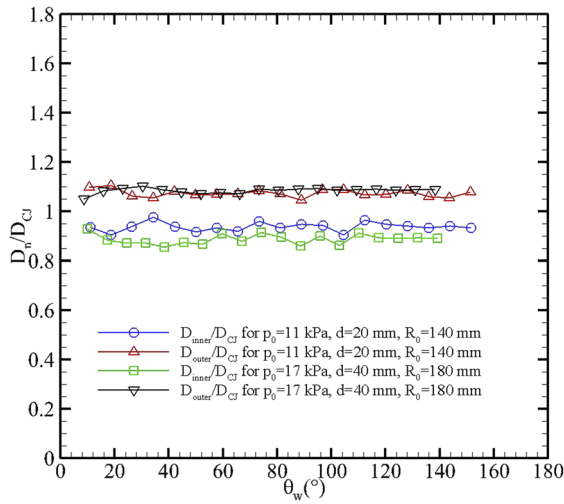


FIG. 12. Velocity evolution on inner and outer walls for the SPGM mode.

and a small d decreases the radial distance from the outer wall to the inner wall,²⁹ i.e., a large ratio R_0/d shortens the path where the reflection triple-point reaches the inner wall significantly. Therefore, the triple-point may possibly reach the inner wall before the diffracted detonation wave decoupled completely, and the detonation wave can thus propagate stably. (2) If the diffracted detonation wave can propagate stably without decoupling as it continues to evolve, then this mode only requires that the reflection triple-point can reach the inner wall in the propagation. It can be found from the density schlieren that in this mode, the detonation wave is actually a Mach-stem formed by the reflection triple-point, which collides repeatedly between two walls. Since the Mach-stem is basically straight, and this mode generally corresponds to the condition of small d with large R_0 , the wave front is roughly planar and perpendicular to the inner and outer walls. The soot foil shows regular cellular patterns with only a slight size variation.

The velocity evolution for the SPGM mode is plotted in Fig. 12. Since a stable propagation is formed, the velocity on both the walls behaves smoothly and remains steady. Although it is ubiquitous that the velocity D_{inner} is lower and D_{outer} is higher than D_{CJ} , the plane

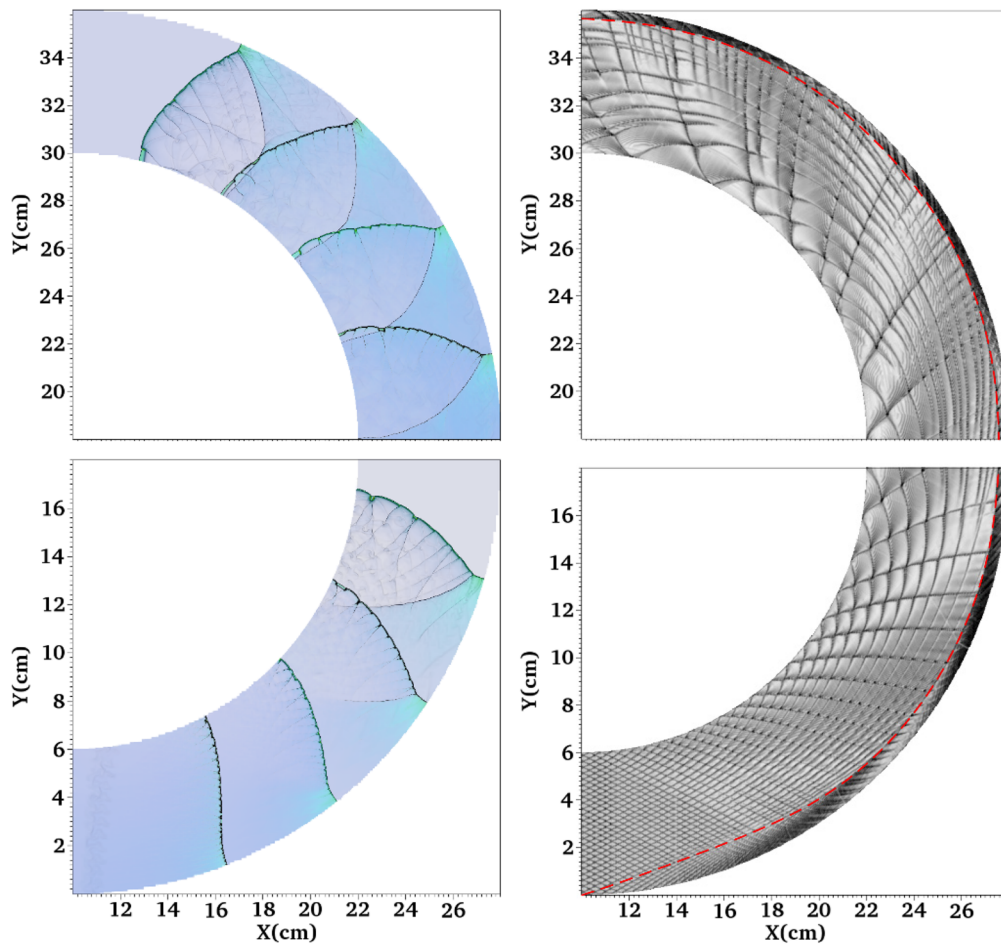


FIG. 13. Density schlieren and numerical soot foil for the SPSM mode (red dashed line: the trajectory of the Mach reflection triple-point).

detonation wave front, which is perpendicular to the walls, makes the velocity ratio D_{inner}/D_{CJ} and D_{outer}/D_{CJ} very close to 1 and leads to a small phase difference between the two velocities. Taking the conditions above as an example, the average value for D_{inner}/D_{CJ} is 0.94 with a maximum variation of 3.9%, and that for D_{outer}/D_{CJ} is 1.07 with a maximum variation of 3.1%, indicating that the velocity evolution is much more stable compared with that in the unstable propagation mode.

2. Stable propagation with steady Mach-stem mode

Figure 13 presents the detonation structure for the stable propagation with steady Mach-stem (SPSM) mode, corresponding to the conditions of $p_0 = 25$ kPa, $d = 60$ mm, and $R_0 = 120$ mm. Compared with the UPSM mode, the diffracted detonation near the inner wall can sustain coupling due to the higher initial pressure p_0 , which ensures that the entire detonation wave propagates stably. Meanwhile, the specific angle between the wave front and the outer wall θ_d keeps the height of the Mach-stem steady. In this mode, the stabilized detonation wave structure is the combination of a curved wave front and a straight Mach-stem, and this structure remains constant in the entire propagation process. Correspondingly, an obvious trajectory of the Mach reflection triple-point can be observed in the soot foil (red line), and the trajectory is parallel to the walls. Compared with the normal detonation cells, the cellular patterns at the left side are generally larger for the rarefaction effect, while the cell sizes on the other side are smaller for the compression effect.

The velocity evolution for the SPSM mode is also relatively steady when the propagation is stabilized, as shown in Fig. 14. However, the differences between the velocities on the walls and D_{CJ} are larger than that in the SPGM mode. For the conditions in this case, the average values for D_{inner}/D_{CJ} and D_{outer}/D_{CJ} are 0.84 and 1.24, respectively. Based on the $D_n - \kappa$ theory,^{20,35–37} the curvature of

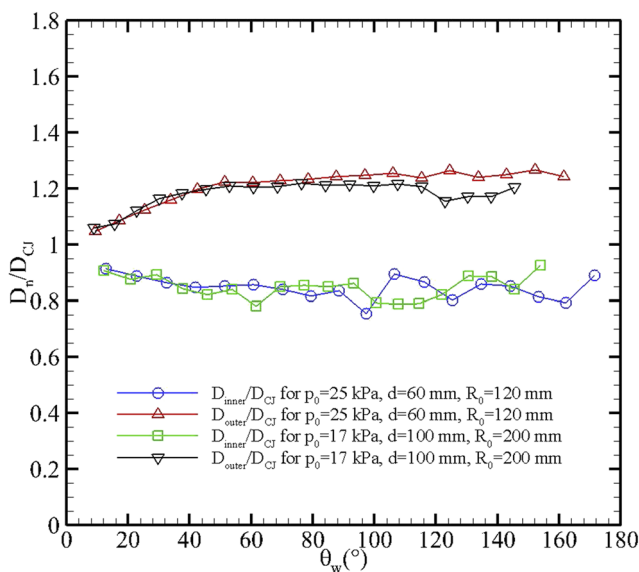


FIG. 14. Velocity evolution on inner and outer walls for the SPSM mode.

detonation wave front will cause the reduction of propagation velocity, which is supposed to be the reason leading to lower velocity on the inner wall, while the decline of the angle θ_d promotes the overdriven state on the outer wall. In addition, since the stabilized structure of the wave front is constant, the phase difference between D_{inner} and D_{outer} is equivalent.

3. Stable propagation with decaying Mach-stem mode

Figure 15 displays the density schlieren and soot foil for the stable detonation propagation with decaying Mach-stem (SPDM) mode, and the corresponding conditions are $p_0 = 25$ kPa, $d = 100$ mm, and $R_0 = 80$ mm. The formation mechanism of this mode is found to be similar to the SPSM mode, the high enough p_0 leads to the diffracted detonation wave propagating stably without decoupling, while the ratio R_0/d is smaller than that of the SPSM mode, thus bending the detonation wave front severely and reducing the angle θ_d . The decreased θ_d causes the decaying of the Mach-stem, and eventually, the Mach reflection is transformed to regular reflection, with the vanishing of the Mach-stem. It can be observed that the stabilized detonation wave is a complete curved front, and the shape can remain constant in the propagation. The trajectory of the Mach reflection triple-point intersects with the outer wall and disappears in the soot foil, indicating that the regular reflection is formed.

The velocity evolution for the SPDM mode is shown in Fig. 16. Although the wave velocity variation on the inner wall is basically stable, some small oscillations can still be observed at the end of the propagation. By combining the soot foil, it is found that the oscillations correspond to the position where the large cells are located, indicating that the oscillations are caused by the collisions between the inner wall and the transverse waves with large space intervals. The average value of D_{inner}/D_{CJ} is 0.78 for the conditions above. As to the outer wall, the stabilized velocity ratio D_{outer}/D_{CJ} reaches 1.8 because of the small angle θ_d caused by the regular reflection.

From the analysis of all the propagation modes above, it can be summarized that in all the unstable propagation modes, the detonation wave near the inner wall is affected by the diffraction, which gives rise to unsteady development, such as decoupling and re-initiation. As a result, the velocity presents strong oscillation with sharp decline and rise. By contrast, the velocities of the stable propagation modes distribute steadily on both walls, which can realize relatively constant rotating propagation frequency. The overdriven degree near the outer wall increases as the Mach-stem attenuates, especially for the Mach-stem decaying type. The regular reflection is eventually formed on the outer wall, thus causing the overdriven degree much larger than other types. Considering the stable work and abundant use of fuel in the RDE, the SPGM mode is supposed to be the most reasonable propagation mode in the combustion chamber for the steadiest velocity behavior and smallest phase difference.

C. Limits of different propagation modes

The propagation mode diagrams with various p_0 , d , and R_0 are plotted in Fig. 17. It should be denoted that considering the large calculation quantity, the Tianhe-2 supercomputer system was adopted and 480 central processing unit (CPU) cores were used to ensure

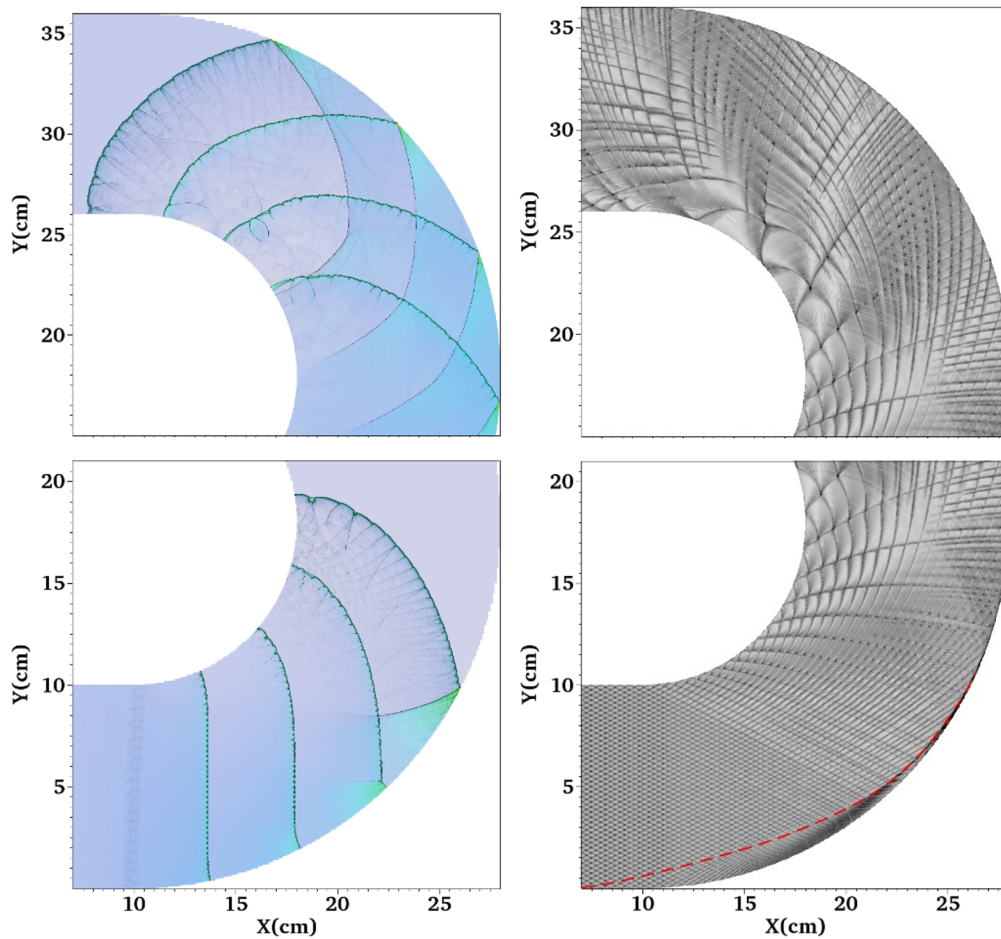


FIG. 15. Density schlieren and numerical soot foil for the SPDM mode (red dashed line: the trajectory of the Mach reflection triple-point).

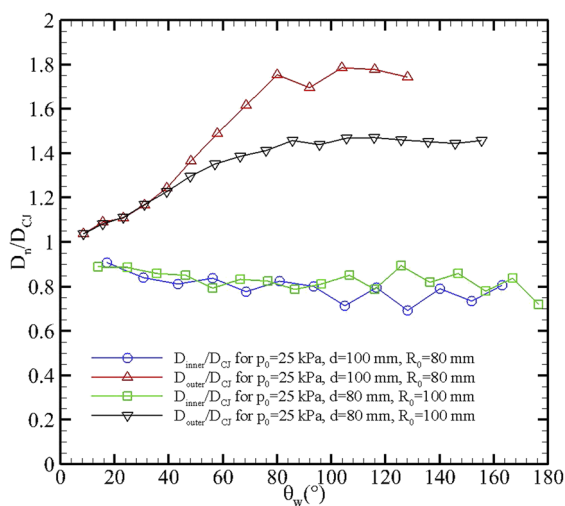


FIG. 16. Velocity evolution on inner and outer walls for the SPDM mode.

the simulations of multiple cases can be conducted parallelly. From the distribution, some basic trends can be deduced. For the unstable and stable mode transformation, which is determined by the diffraction near the inner wall, the increase of p_0 enhances the sensitivity of the detonation wave to prevent the wave front from decoupling, so the range of the stable propagation mode is extended, which agrees with the previous studies.^{14,15} With the increase in R_0 , the propagation mode is also transformed from the unstable to stable type, for that the rarefaction effect of the diffraction is weakened. While the mode transition between unstable and stable seems to have no obvious relation with the channel width d . As to the types of the Mach-stem evolution, which are dominated by the reflection at the side of the outer wall, with the increase in p_0 , the Mach-stem has the transformation tendency from growing to steady and then to decaying mode. The reason is that the increase of p_0 shortens the length of both the induction and reaction zones, accelerating the attenuation of the Mach-stem, which has also been reported in the previous study.²⁹ The increase of R_0 can enlarge the Mach-stem height at the same center angle θ_w , while the decrease of d_0 can shorten the radial distance between the two walls, so the Mach-stem develops

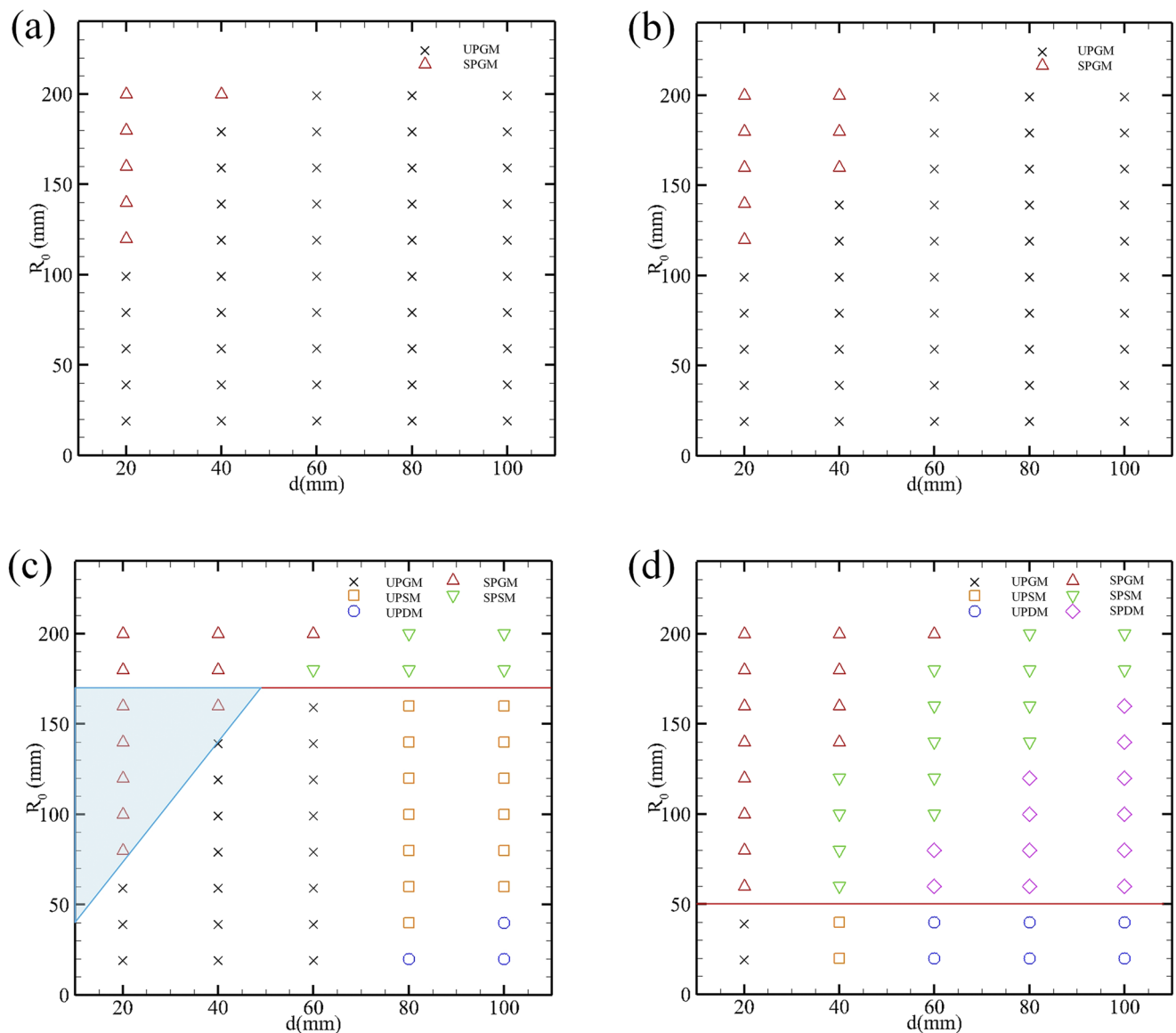


FIG. 17. Distribution of the detonation propagation mode for all simulation cases: (a) $p_0 = 6.5$ kPa, (b) $p_0 = 11$ kPa, (c) $p_0 = 17$ kPa, and (d) $p_0 = 25$ kPa.

from decaying to steady to growing with the increase in the ratio R_0/d_0 .

Further analysis of the transformation boundaries between different propagation modes indicates that for the steady and decaying Mach-stem types, the boundary value of R_0 between the unstable and stable propagation modes seems to be independent of d_0 [see the red line in Figs. 17(c) and 17(d)]. It can be explained that the unstable or stable mode is mainly determined by whether the diffracted detonation wave near the inner wall can propagate stably without decoupling, and it has been proven that the stable propagation of the diffracted detonation wave has no relation with d_0 .²⁸ However, for the growing Mach-stem type, some cases with the SPGM mode

distribute in the range where the diffracted detonation wave cannot sustain stable propagation [see the blue shaded area in Fig. 17(c)], and the boundary value of R_0 for these cases increases with the increase in d_0 . These cases indeed correspond to the situation where the reflection triple-point reaches the inner wall before the diffracted detonation wave decoupled, which has been indicated in Sec. III B 1. As d_0 increases, the reflection triple-point should move a longer distance to reach the inner wall, so a larger R_0 is needed to delay the decoupling of the detonation wave and form stable propagation.

Finally, Fig. 18 shows a flowchart outlining a procedure to distinguish different mode transformations and limits based on the

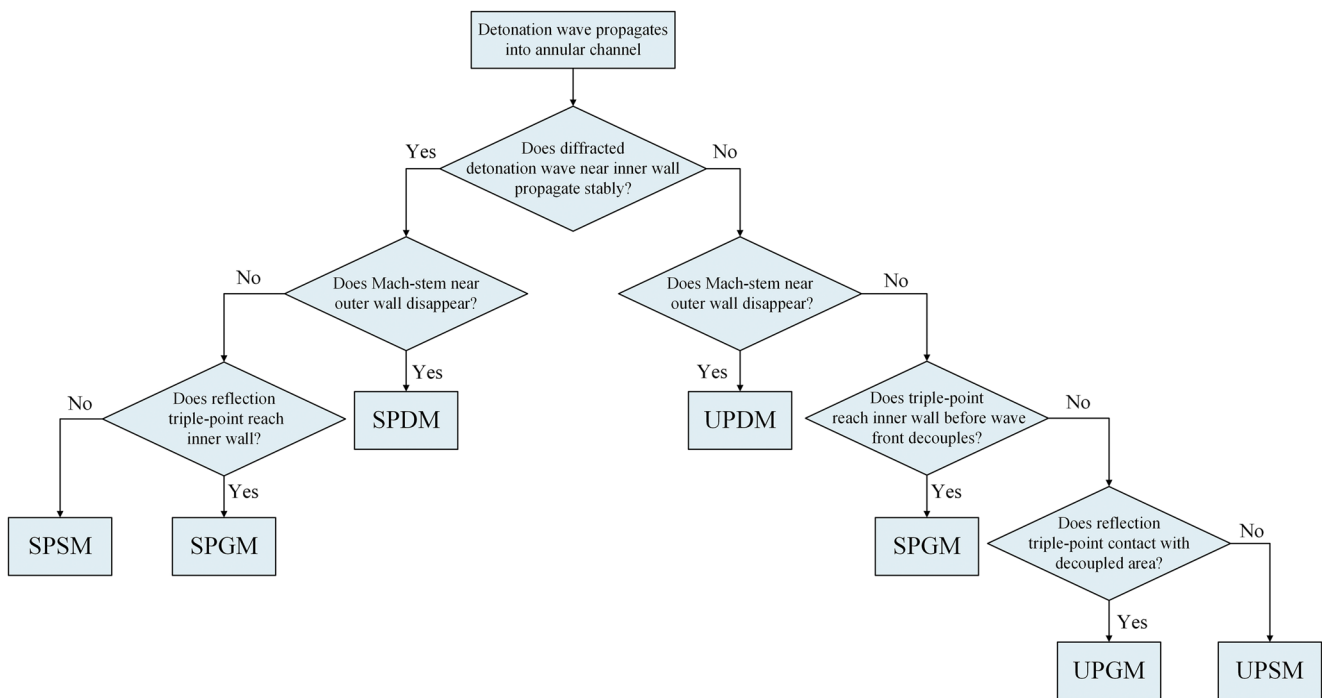


FIG. 18. A flowchart showing the procedure for distinguishing transformation of different propagation modes.

formation mechanism of each propagation mode. If the critical conditions at which each of the above physical processes occurs can be determined theoretically, then the overall propagation mode in a rotating detonation engine can be predicted. This is beyond the scope of this paper and is currently under on-going investigation.

IV. CONCLUSIONS

The dynamics of detonation wave propagation in annular channels were investigated by two-dimensional numerical simulations using the reactive Euler equations with a detailed hydrogen/oxygen reaction model. The detonation wave propagation modes were revealed in detail by considering both the decoupling of the detonation wave front and the development of the reflection Mach-stem. The formation mechanism, wave structure, and velocity on both walls were discussed for each propagation mode. The rule of propagation mode distribution was analyzed, and a procedure to distinguish the propagation mode was constructed based on the formation mechanism.

The detonation wave propagation can be divided into unstable and stable modes according to whether the wave front is decoupled from the diffraction near the inner wall. In the unstable propagation mode, decoupling and re-initiation of the detonation wave will occur alternatively, resulting in velocity loss and oscillation near the inner wall. In contrast, the wave front shape and velocity behavior are steadier for the stable propagation mode.

Following the development of the reflection Mach-stem, the propagation mode can be further divided into three types: growing,

steady, and decaying Mach-stem type. The overdriven degree near the outer wall increases with the attenuation of the Mach-stem, especially for the Mach-stem decaying type, the formation of the regular reflection on the outer wall causes the overdriven degree much larger than other types.

The increase of initial pressure p_0 can enhance the strength of the detonation wave and extend the range of the stable propagation mode. The propagation mode is also transformed from unstable to stable with the increase in the inner wall curvature radius R_0 . The Mach-stem has the transformation tendency from growing to steady to decaying, with the increase in p_0 , while with the increase in the ratio R_0/d_0 , the Mach-stem develops from decaying to steady to growing. The transformation boundary between unstable and stable propagation modes is independent of d_0 for the Mach-stem steady and decaying types. However, for the Mach-stem growing type, the boundary value of R_0 increases with the increase in d_0 .

Based on the formation mechanism of each propagation mode, a procedure is built to distinguish the mode transformation, and all the propagation modes can be predictable if the determining conditions can be expressed mathematically, which needs to be further studied.

ACKNOWLEDGMENTS

This work was supported by the National Natural Science Foundation of China under Grant No. 51776220 and the Key Laboratories Program of China under Grant No. 6142704200101.

DATA AVAILABILITY

The data that support the findings of this study are available from the corresponding author upon reasonable request.

REFERENCES

- ¹S.-J. Liu, Z.-Y. Lin, W.-D. Liu, W. Lin, and M.-B. Sun, "Experimental and three-dimensional numerical investigations on H₂/air continuous rotating detonation wave," *Proc. Inst. Mech. Eng., Part G* **227**, 326 (2013).
- ²S. M. Frolov, V. S. Aksenov, V. S. Ivanov, and I. O. Shamshin, "Large-scale hydrogen-air continuous detonation combustor," *Int. J. Hydrogen Energy* **40**, 1616 (2015).
- ³Y. Liu, W. Zhou, Y. Yang, Z. Liu, and J. Wang, "Numerical study on the instabilities in H₂-air rotating detonation engines," *Phys. Fluids* **30**, 046106 (2018).
- ⁴J. Koch and J. N. Kutz, "Modeling thermodynamic trends of rotating detonation engines," *Phys. Fluids* **32**, 126102 (2020).
- ⁵H. Zhang, W. Liu, and S. Liu, "Effects of inner cylinder length on H₂/air rotating detonation," *Int. J. Hydrogen Energy* **41**, 13281 (2016).
- ⁶G. O. Thomas and R. L. Williams, "Detonation interaction with wedges and bends," *Shock Waves* **11**, 481 (2002).
- ⁷R. Deiterding, "A parallel adaptive method for simulating shock-induced combustion with detailed chemical kinetics in complex domains," *Comput. Struct.* **87**, 769 (2009).
- ⁸R. Deiterding, "High-resolution numerical simulation and analysis of Mach reflection structures in detonation waves in low-pressure H₂-O₂-Ar mixtures: A summary of results obtained with the adaptive mesh refinement framework AMROC," *J. Combust.* **2011**, 738969.
- ⁹J. Li, H. Ren, and J. Ning, "Numerical application of additive Runge-Kutta methods on detonation interaction with pipe bends," *Int. J. Hydrogen Energy* **38**, 9016 (2013).
- ¹⁰X. Yuan, J. Zhou, Z. Lin, and X. Cai, "Adaptive simulations of detonation propagation in 90-degree bent tubes," *Int. J. Hydrogen Energy* **41**, 18259 (2016).
- ¹¹J. Melguizo-Gavilanes, V. Rodriguez, P. Vidal, and R. Zitoun, "Dynamics of detonation transmission and propagation in a curved chamber: A numerical and experimental analysis," *Combust. Flame* **223**, 460 (2021).
- ¹²E. Ioannou, S. Schoch, N. Nikiforakis, and L. Michael, "Detonation propagation in annular arcs of condensed phase explosives," *Phys. Fluids* **29**, 116102 (2017).
- ¹³S. Lee, D. R. Cho, and J. Y. Choi, "Effect of curvature on the detonation wave propagation characteristics in annular channels," in *the 46th AIAA Aerospace Sciences Meeting and Exhibit* (AIAA, 2008).
- ¹⁴Y. Kudo, Y. Nagura, J. Kasahara, Y. Sasamoto, and A. Matsuo, "Oblique detonation waves stabilized in rectangular-cross-section bent tubes," *Proc. Combust. Inst.* **33**, 2319 (2011).
- ¹⁵H. Nakayama, T. Moriya, J. Kasahara, A. Matsuo, Y. Sasamoto, and I. Funaki, "Stable detonation wave propagation in rectangular-cross-section curved channels," *Combust. Flame* **159**, 859 (2012).
- ¹⁶H. Nakayama, T. Moriya, J. Kasahara, A. Matsuo, and I. Funaki, "Front shock behavior of stable detonation waves propagating through rectangular cross-section curved channels," in *the 50th AIAA Aerospace Sciences Meeting including the New Horizons Forum and Aerospace Exposition* (AIAA, 2012).
- ¹⁷H. Nakayama, J. Kasahara, A. Matsuo, and I. Funaki, "Front shock behavior of stable curved detonation waves in rectangular-cross-section curved channels," *Proc. Combust. Inst.* **34**, 1939 (2013).
- ¹⁸Z. Pan, J. Qi, J. Pan, P. Zhang, Y. Zhu, and M. Gui, "Fabrication of a helical detonation channel: Effect of initial pressure on the detonation propagation modes of ethylene/oxygen mixtures," *Combust. Flame* **192**, 1 (2018).
- ¹⁹Z. Pan, K. Chen, J. Qi, P. Zhang, Y. Zhu, J. Pan, and M. Gui, "The propagation characteristics of curved detonation wave: Experiments in helical channels," *Proc. Combust. Inst.* **37**, 3585 (2019).
- ²⁰Y. Sugiyama, Y. Nakayama, A. Matsuo, H. Nakayama, and J. Kasahara, "Numerical investigations on detonation propagation in a two-dimensional curved channel," *Combust. Sci. Technol.* **186**, 1662 (2014).
- ²¹M. Short, C. Chiquete, and J. J. Quirk, "Propagation of a stable gaseous detonation in a circular arc configuration," *Proc. Combust. Inst.* **37**, 3593 (2019).
- ²²Z. Xia, H. Ma, C. Zhuo, and C. Zhou, "Propagation process of H₂/air rotating detonation wave and influence factors in plane-radial structure," *Int. J. Hydrogen Energy* **43**, 4609 (2018).
- ²³C. K. Westbrook, "Chemical kinetics of hydrocarbon oxidation in gaseous detonations," *Combust. Flame* **46**, 191 (1982).
- ²⁴R. Deiterding, "Parallel adaptive simulation of multi-dimensional detonation structures," Ph.D. thesis, Brandenburgische Technische Universität Cottbus, 2003.
- ²⁵M. J. Berger, "Adaptive mesh refinement for hyperbolic equations," in *Large-Scale Computations in Fluid Mechanics, Part 1* (Stanford University, 1982).
- ²⁶H. Peng, Y. Huang, R. Deiterding, Z. Luan, F. Xing, and Y. You, "Effects of jet in crossflow on flame acceleration and deflagration to detonation transition in methane-oxygen mixture," *Combust. Flame* **198**, 69 (2018).
- ²⁷X. Cai, R. Deiterding, J. Liang, M. Sun, and Y. Mahmoudi, "Diffusion and mixing effects in hot jet initiation and propagation of hydrogen detonations," *J. Fluid Mech.* **836**, 324 (2018).
- ²⁸X. Yuan, J. Zhou, S. Liu, and Z. Lin, "Diffraction of cellular detonation wave over a cylindrical convex wall," *Acta Astronaut.* **169**, 94 (2019).
- ²⁹X. Yuan, J. Zhou, X. Mi, and H. D. Ng, "Numerical study of cellular detonation wave reflection over a cylindrical concave wedge," *Combust. Flame* **202**, 179 (2019).
- ³⁰C. Lin and K. H. Luo, "Mesoscopic simulation of nonequilibrium detonation with discrete Boltzmann method," *Combust. Flame* **198**, 356 (2018).
- ³¹C. Lin and K. H. Luo, "Discrete Boltzmann modeling of unsteady reactive flows with nonequilibrium effects," *Phys. Rev. E* **99**, 012142 (2019).
- ³²Y. Ji, C. Lin, and K. H. Luo, "Three-dimensional multiple-relaxation-time discrete Boltzmann model of compressible reactive flows with nonequilibrium effects," *AIP Adv.* **11**, 045217 (2021).
- ³³E. Hairer and G. Wanner, *Solving Ordinary Differential Equations II: Stiff and Differential-Algebraic Problems* (Springer, Berlin, Heidelberg, 1996).
- ³⁴X. Q. Yuan, X. C. Mi, H. D. Ng, and J. Zhou, "A model for the trajectory of the transverse detonation resulting from re-initiation of a diffracted detonation," *Shock Waves* **30**, 13 (2020).
- ³⁵W. W. Wood and J. G. Kirkwood, "Diameter effect in condensed explosives. The relation between velocity and radius of curvature of the detonation wave," *J. Chem. Phys.* **22**, 1920 (1954).
- ³⁶S. D. Watt and G. J. Sharpe, "Linear and nonlinear dynamics of cylindrically and spherically expanding detonation waves," *J. Fluid Mech.* **522**, 329 (2005).
- ³⁷H. Soury and K. Mazaheri, "Utilizing unsteady curved detonation analysis and detailed kinetics to study the direct initiation of detonation in H₂-O₂ and H₂-Air mixtures," *Int. J. Hydrogen Energy* **34**, 9847 (2009).